

Transport barrier formation and its maintenance by LHCD on TRIAM-1M

K.HANADA¹⁾, A.IYOMASA¹⁾, H.ZUSHI¹⁾, M.HASEGAWA¹⁾, K.SASAKI¹⁾, H.HOSHIKA¹⁾,
K.NAKAMURA¹⁾, S.SHIRAIWA²⁾, M.SAKAMOTO¹⁾, K.N.SATO¹⁾, H.IDEI¹⁾,
S.KAWASAKI¹⁾, H.NAKASHIMA¹⁾, and A.HIGASHIJIMA¹⁾

- 1) Advanced Fusion Research Center, Research Institute for Applied Mechanics, Kyushu University, Kasuga 816-8580, Fukuoka, Japan
- 2) Grad. School of Frontier Sciences and Grad. School of Science, Univ. Tokyo, Chiba 277-8561, Japan

E-mail:hanada@triam.kyushu-u.ac.jp

Abstract: Internal transport barrier (ITB) has been obtained in full lower hybrid current driven (LHCD) plasmas on a superconducting tokamak, TRIAM-1M ($R=0.84\text{m}$, $a \times b=0.12\text{m} \times 0.18\text{m}$, $B_T < 8\text{T}$). This discharge is classified with the enhanced current drive (ECD) mode, because the current drive efficiency is spontaneously increasing during the discharge. The formation of ITB is caused by the reduction of the lower hybrid (LH) power deposited at the center of plasma. The plasma with ITB can be maintained by the LH power deposited around the foot point of ITB up to 25 sec, which corresponds to more than 100 times of current diffusion time, $\tau_{L/R}$. This indicates that the formation of ITB has the relation to the current density at the foot point of ITB. Self-organized slow sawtooth oscillations (SSSO) of plasma current, density, temperature, and so on with the period comparable to the current diffusion time have been also observed in long duration full LHCD discharges. The oscillation, which has no helical structure, appears only in the high performance plasma with ITB and it seems to be induced by the variation of the transport coefficient which has relation to the current density profile estimated by the radiation from energetic electrons. A crash is sometimes accompanied by the predator prey type instability related with ITB and the decay time of the density is comparable to the energy confinement time. Taking place a crash, particles accumulated inside ITB are released to the peripheral region of the plasma and consequently the plasma is possible to recover the high performance condition with the time constant of $\tau_{L/R}$. The action of particle exhaust caused by SSSO is preferable to maintain the high performance condition, because the transition to the high performance plasma under the high influx of metal impurities can be obtained and it may play an role in the avoidance of the impurity accumulation and the dilution in the future steady state fusion plasma with ITB, as the edge-localized mode in H-mode.

1. Introduction

Steady state operation of high performance plasma is one of the key issues to realize cost-effective fusion power plant. High performance plasma with the transport barrier is a good candidate from the view of plasma confinement [1-7]. Especially it is important that the high performance plasma was maintained by fully non-inductive current drive. Some experimental observations have been shown to achieve the good performance plasma for the longer duration than the current diffusion time [8, 9]. Many studies of internal transport barrier (ITB) were carried out in many devices and it was found that ITB is common phenomena [10-13]. In tokamak plasmas, transport coefficients have strong relation to current density profile, that is magnetic shear [4, 5], and the current profile control is important tool for the control the performance of the plasma. Especially lower hybrid current drive (LHCD) is powerful tool for the control of current profile and in fact some experiments show the promising possibility [14, 15].

With the reduction of the transport coefficient, the capability to accumulate impurities [16, 17] and He ash produced by the fusion reaction in the core region will be growing. The accumulated impurities lead to the huge energy loss in the core region via strong radiation and the He ash brings to the dilution of the fuel for fusion reaction. These are the serious problem to adopt the plasma with transport barrier as the core plasma in fusion power plant. Thus the investigation of the scenarios to exhaust impurities and He ash from the core to the peripheral region is important. As H-mode, which has the edge transport barrier (ETB), has the scenario to exhaust He ash and impurities accumulated into the core plasma via self-organized action of Edge localized mode (ELM), the standard operation of ITER was decided as ELM'y H-mode operation. ELM is one of the MHD phenomena and it plays an essential role in the

exhaust of He ash and impurities to the peripheral region of the plasma intermittently.

Recently, self-organized sinusoidal oscillation could be observed in long duration plasma maintained by fully non-inductive LHCD on Tore Supra [18]. This oscillation could be understood as a predator-prey instabilities derived from the variation of the transport coefficient related to current density profile as the following. The power deposition of LHCD depends on the electron temperature and the electron temperature is controlled by the transport coefficient related to current density profile. The relation was formed a predator-prey relation and as the result the oscillation in the electron temperature and current density profile appears in core region of the non-inductive long duration discharge. The growth rate of the oscillation is zero and there are no effects in the exhaust of the accumulated impurities and it may not play an essential role in the particle exhaust of the plasma with ITB [18].

On TRIAM-1M [19], the formation of ITB and the oscillation related with ITB formation has been obtained in ECD plasmas [20-22]. The plasma with ITB can be maintained by the LH power deposited around the foot point of ITB up to 12 sec, which corresponds to more than 50 times of current diffusion time, $\tau_{L/R}$. The oscillation has the capability for the exhaust of the particles including the impurities. In fact, a transition to high performance plasma with ITB could be achieved under the high influx of impurities.

In section 2, the brief introduction of the experimental apparatus is shown and the experimental results concerning the formation of ITB is described in section 3 and consequently the results of the oscillation related ITB formation is shown in the section 4. The summary is described in the section 5.

2. Experimental Apparatus

TRIAM-1M ($R=0.84\text{m}$, $a \times b=0.12\text{m} \times 0.18\text{m}$) is a small size high magnetic field tokamak with 16 superconducting toroidal magnetic field coils made of Nb_3Sn , which produces the toroidal magnetic field, B_T , up to 8T in steady state. A 2.45GHz LHCD system, which has a klystron (2.45GHz, maximum power = 50kW), two 8.2 GHz LHCD systems, which have 8 klystrons (8.2GHz, maximum power = 25kW per a klystron), and an electron cyclotron heating (ECH) system, which has a gyrotron (170 GHz, maximum power = 200kW) are installed on TRIAM-1M as additional heating sources. Experiments described in this paper are carried out by two 8.2 GHz LHCD systems.

Source microwave generated by DIO has been divided by 2 branches at first. One branch is source microwave for a system and another one is for another system. Each source microwave has been divided by 8 branches and transmitted through a phase shifter driven by a motor and an attenuator in each branch. Microwave amplified by an 8.2 GHz klystron up to 25 kW has been transmitted by water-cooled waveguides with rectangle cross-section. High power microwave has been divided by 2 branches. One branch has a phase shifter for high power microwave. High power microwave in each system has been injected into plasma through an 8x2 grill type launcher from low field side and lower hybrid wave (LHW) is excited in the plasma. The phase velocity of the excited LHW can be varied by the phase difference in the adjacent waveguide of the launcher, which is controlled by the phase shifter described above. One system (System_1) has the capability to change the power during the discharge and change the phase velocity of LHW shot by shot. Another system (System_2) has the capability to control the phase velocity of LHW during a discharge with 10 degree per a second as well as the power. When the reflected power is over a certain level, the power of microwave is stopped immediately to avoid the break of vacuum windows, which is made of thin sapphire cooled by water in each system.

Main diagnostics in this paper are a soft X-ray (SXR) detector array composed of 19ch silicon surface barrier (SSB) diodes sensitive to photon in the range of 0.07keV-30keV and a hard X-ray (HXR) detector array composed of 7ch NaI scintillators sensitive to photon with 40-500keV. Low energy part of HXR is absorbed by the vacuum window made of Aluminum.

The NaI scintillators have been arranged along the major radius. The viewing chord sets to the perpendicular direction to the toroidal magnetic field

3. The formation of internal transport barrier

Typical waveforms of the discharge with ITB are shown in Fig.1. The time slices of the profile of soft X-Ray are also shown in Fig.1. The plasma was maintained by the combination of two LH waves with the different phase velocity controlled by the phase difference of the adjacent waveguide at the launcher. All of the plasma current was driven by these LH power non-inductively at any time except the start-up phase of the discharge. The LH power of System_1 was gradually raised from 3 s to 3.5s by 50kW. As the result, both plasma current and electron density follow the increase of injected LH power. In this duration, the current drive efficiency did not change with that before the increment of the LH power of System_1. From 3.5s, the LH power of the System_2 is gradually reduced and the abrupt increase of the electron density can be observed around 4.2s. At that time, the profile of SXR Intensity, I_{SX} , is also peaked as shown in Fig. 1 and the current drive efficiency is also improved. When the LH power of System_2 is not reduced, the peaked I_{SX} profile is not obtained. While the LH power of System_1 is not raised, the peaked I_{SX} profile is not also obtained. These results show that the LH power of System_1 assists the formation of the peaked I_{SX} profile and that of System_2 obstructs it. The peaked I_{SX} profile shows that the electron pressure is peaked as shown in the rapid increase of electron density. When the peaked I_{SX} profile is formed, the total of the injected LH power to the plasma is reduced. This shows that the peaked electron pressure is not made by the increment of the deposited power to the center of the plasma, but by the reduction of transport coefficient around $r=5$ cm, where is around the foot of ITB in the plasma. The ion temperature, T_i , at the center of the plasma also increases, and it means that the ion transport also become to be better.

After the transition, the LH power of System_1 is gradually reduced and the back-transition takes place around 7 s. After the back-transition, n_e and I_p return to the previous levels and finally the further reduction of the LH power makes the termination of the plasma. The LH power required to maintain the plasma current is about 30kW.

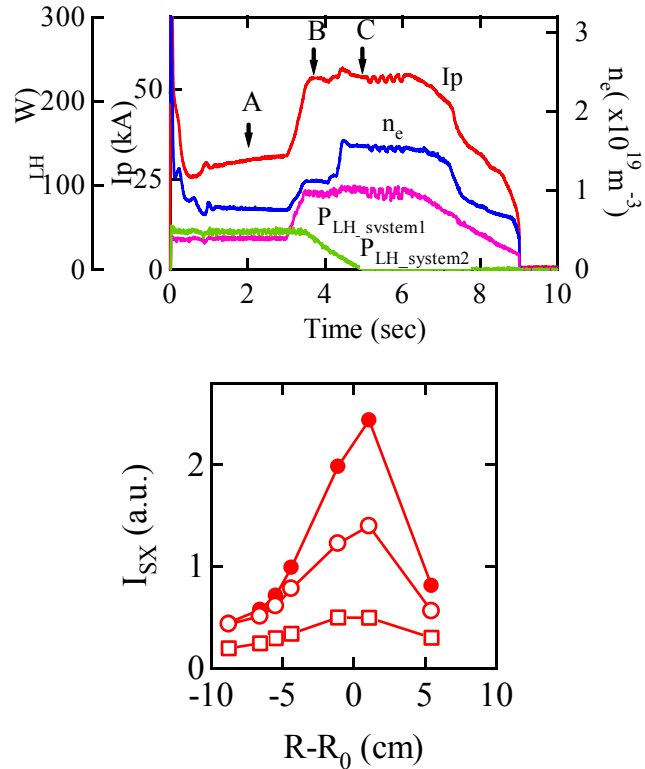


Fig.1 Time evolution of plasma current (red line), electron density (Blue line), LH power of System_1 (pink line) LH power of System_2 (green line) are plotted in the upper figure. The profiles of soft X-ray intensity at the time marked as A (open squares), B (open circles) and C (closed circles) in the upper figure are shown in the lower figure.

To investigate the difference of the effect of each LH power to the plasma, the modulation of the LH power during the discharge was carried out. The LH power modulation was executed from 5s to 6s as shown in Fig. 1. The LH power was modulated every 100ms by 15% of the power. The plasma current and electron density were also modulated as shown in Fig.1. The intensities of HXR, I_{HX} , correspond to the signal of the pressure of tail electrons around 40keV. It is noted that I_{HX} is also proportional to the bulk electron density and Z_{eff} . To remove the effect of electron density and Z_{eff} profile to I_{HX} signal, the inversed decay time, $1/I_{HX}dI_{HX}/dt$ is calculated at first and the inversed decay times is multiplied by energy stored of tail electrons. Thus the power deposition of LHW are calculated and they are plotted as the function of minor radius as shown in Fig.2. The power deposition of System_1 is mainly deposited at the position of $r=5\text{cm}$ in any cases, it suggests that the LH power of System_1 is mainly deposited at the position of $r=5\text{cm}$ and it plays a role in making broad current profile. While the LH power of System_2 is deposited at the center of plasma and it makes peaked current profile. This suggests that the formation of ITB is assisted by the LH current drive at the foot point of ITB.

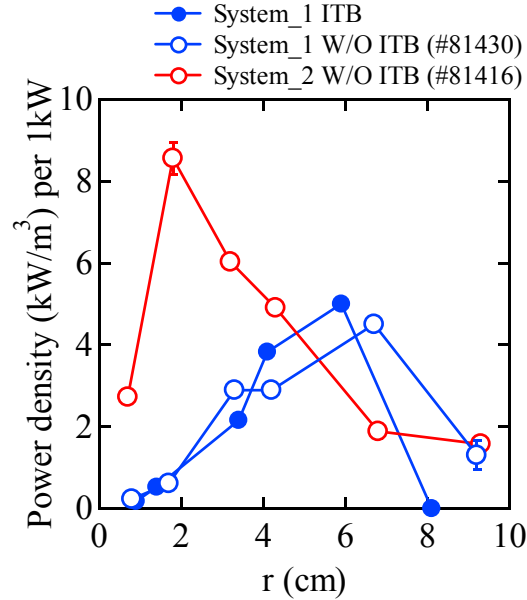


Fig.2 Power deposition profile of System_1 with ITB (closed blue circles), System_1 without ITB (open blue circles), and System_2 without ITB (open red circles) during the LH power modulation experiment are plotted as the function of minor radius.

The long duration discharge with ITB by use of only System_1 can be achieved up to 25 s, which corresponds to 100 times of current diffusion time, $\tau_{L/R}$. A back-transition takes place during the discharge, and the discharge can be maintained by LHCD for 36 sec. The influx of ferrite estimated by the line intensity of FeI increases during the discharge gradually. In the other discharge, just before the termination of ITB, a number of grains of Molybdenum put into the plasma and plasma performance become to be worse. The grains come from the poloidal limiter made of Molybdenum. The time evolution of the line intensity of Mo XIII inversely synchronizes with that of the plasma current. These indicate that the metal impurity accumulation plays an essential role in the back-transition from high performance plasma with ITB.

4. Self-organized Oscillation related with ITB

The new kind of self-organized slow sawtooth oscillation (SSSO) has been observed in long-duration fully non-inductive LHCD plasmas. SSSO has been obtained only in high performance plasma with ITB. The period of the oscillation is comparable to the current diffusion time, $\tau_{L/R}$, of the plasma (a few hundreds ms). The crashes of SSSO is sometimes accompanied by precursor, which is similar to the predator-pray instability observed in Tore Supra. This precursor has no helical structure and the period is similar to the change of the current profile (a few tens ms).

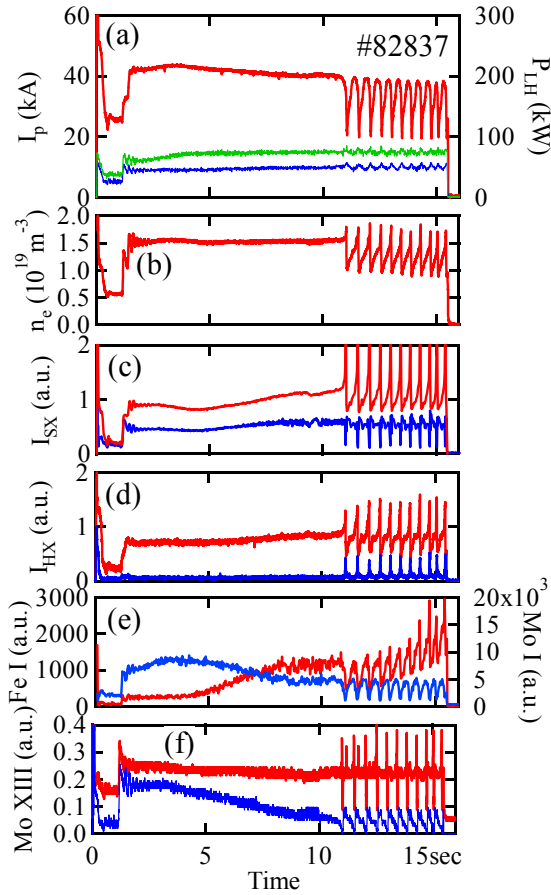


Fig. 3 The typical waveforms of (a) plasma current, I_p and the net injected LH power, P_{LH} , (b) electron density, n_e , (c) Intensity of SXR at $r=0\text{cm}$ (red line) and 7.8cm (blue line), (d) Intensity of HXR at $r=0\text{cm}$ (red line) and 5cm (blue line), (e) Photon count of FeI (red line) and MoI (blue line), and (f) VUV signal of MoXIII at $r=2.5\text{cm}$ (red line) and 5cm (blue line).

hard X-ray (HXR) at the center of the plasma also burgeons as shown in Fig. 3(d). This suggests that ITB of n_e is formed, rather than T_e . The formation of ITB has the strong relation to the LH power [20] and $N_{||}$ [21]. With the reduction of $N_{||}$, the deposition of LHW is far from the center of plasma and the current drive efficiency, η_{CD} , degrades. When the value of $N_{||}$ of the additional LHW sets to more than 2.4, ITB is not able to be achieved. It is found that the power deposited at the center of the plasma prevents from forming ITB, where the power deposition can be measured with the variation of HXR during the power modulation. This shows that the formation of ITB depends on the current profile driven by the injected LHW. The RF power of $N_{||}=1.8$ mainly deposits at the ITB foot ($r/a=0.5$).

The plasma current is reduced gradually, because the reduction of η_{CD} occurs due to the shift of the $N_{||}$ from 2 to 4 sec. Since 4 sec, the reduction of η_{CD} seems to be derived from the increase of Z_{eff} . The intensity of FeI (I_{FeI}), which is proportional to the influx of ferrite, increases gradually as shown in Fig. 3(e) and simultaneously the intensity of MoI (I_{MoI}) is reduced, where the values of I_{FeI} and I_{MoI} is measured with a spectroscopy viewing the movable limiter from the bottom port of #1. Ferrite come from the movable limiter installed

The typical waveforms of the plasma parameters are shown in Fig. 3. The plasma current is maintained by lower hybrid wave (LHW) of the peak $N_{||}=1.8$ excited by System_1, where $N_{||}$ is the refractive index along the magnetic field line. From the beginning of plasma, the additional LHW excited by another LHCD device of the frequency in 8.2GHz is injected into the plasma. The value of $N_{||}$ of System_2 is shifted from 1.8 (0-2sec) to 2.0 (4sec-the end of the discharge) during the discharge. The net injection power of RF increases at 1.2 sec because of the improvement of the coupling between microwave and the plasma, and as the result the first jump of I_p and n_e occurs around 1.2 sec as shown in Figs. 3(a) and (b), where the relative intensity between SXR emitted at the center chord and at the peripheral chord does not change so much as shown in Fig. 3(d). The second jump of I_p and n_e is observed around 1.5sec, although the net LH power does not change [20-22]. At the second jump, the intensity (I_{SX}) of SXR at the center chord burgeons and that at the peripheral chord decreases slightly. This shows that the formation of steep gradient of n_e and electron temperature, T_e , occurs at the time of the second jump, which shows the formation of ITB in the plasma. The position of ITB foot is estimated by the profile of SXR and it locates around $r=6\text{ cm}$ ($r/a=0.5$), where r and a are the distance between line of sight and the plasma center and minor radius of the plasma, respectively. The intensity (I_{HX}) of

on the upper part of #1 port. Energetic electrons produced by LHW are directly attacked to the movable limiter. The movable limiter is made of SS covered by Molybdenum. The energy and orbit of the energetic electrons depends on the value of $N_{//}$. The waveform of the intensity of Mo XIII (I_{MoXIII}) outside of the ITB region is reduced and it is similar to I_{MoI} . However I_{MoXIII} around the ITB foot does not decrease as shown in Fig. 3(f). This indicates that the metal impurities accumulate in the core region as reported in the other devices [10, 11]. Unfortunately we do not measure the radiation of the ferric ion. However ferric ion will accumulate more inside ITB because of the increase of the influx of ferrite as shown in Fig. 3(e). Surely the intensity of SXR at the center of the plasma suggests that the value of Z_{eff} gradually increases.

Around 11 sec, an oscillation appears in plasma current, density and so on as shown in Fig. 3. The periods of the oscillation is in the range of a few hundreds ms and it corresponds to the current diffusion time ($\sim 200\text{ms}$) of the plasma. This oscillation occurs in the self-organized manner and the oscillation is sometimes accompanied by the periodic predator-pray type instabilities observed in Tore Supra [18] just before the crash. The termination of the discharge is not due to the long-duration oscillation, but to the shut-down of the LH power. The time evolutions of n_e and T_i at the center of the plasma are shown in Fig. 4. As soon as the value of T_i starts to be reduced, the value of n_e at the center of the plasma is jumped-up, despite the difference of the sampling frequency. Consequently, the reduction of T_i occurs in the middle way of the increase of n_e and then the bottom value of both parameters seems to come at the same time. The time constant of the reduction of T_i is longer than that of n_e . This result shows that the reduction of ion temperature is caused by the impurity accumulation around the center of plasma.

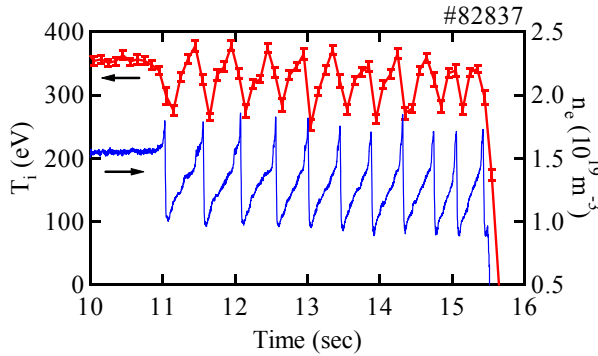


Fig. 4 Typical waveforms of ion temperature at $r=0\text{cm}$ and line-averaged density, n_e around SSSO.

The enlarged figures around a crash without the precursor are shown in Fig. 5. At first, the value of I_p is reduced in Fig. 5(a), and the jump up of the value of n_e and the consequent abrupt reduction are shown in Fig. 5(a). The decay time of n_e (5-10ms) is comparable to energy confinement time, τ_E . The peak value of I_{SX} profile and the value of full width half maximum (FWHM) of I_{SX} profile are shown in Fig. 5(b). The increase of the peak value of I_{SX} can be observed before the crash and the growth time is similar to that of n_e at the plasma center. The value of FWHM of I_{SX} profile gradually

decreases before the crash and since the crash the profile of I_{SX} expands. This shows that the region of ITB is shrinking before the crash and the peak value is increasing. After the crash, the particles and the energy stored inside ITB are released and as the result the intensity of I_{SX} around the peripheral region increases due to the particle and heat flow to the outside of the plasma. The outward particles and energy flow can be recognized by the expansion of I_{SX} profile after the crash. Finally the plasma is willing to recover the formation of ITB in self-organized manner. This indicates that the action of the particle exhaust works during the crash and it assists with the regeneration of ITB.

The time evolutions of the ratio of I_{HX} to I_{SX} at the same radial position is shown in Fig. 5(c). The value of I_{HX}/I_{SX} approximately shows the ratio of the density of energetic electron to the density of bulk electron, because many plasma parameters, Z_{eff} , bulk electron density, and so on, can be canceled by division. The time evolutions of I_{HX}/I_{SX} show that the energetic electrons at the center of the plasma are reduced and that around foot point of ITB increases vice versa, which shows that the current density will make strong negative shear and the transport coefficient become to be improved more. Accordingly, the electron density at the center of the plasma burgeons and it makes strong pressure gradient in the plasma core. Finally, the improved transport coefficient becomes worse by the instabilities enhanced by the strong pressure gradient. This is consistent with the observations that the ITB region shrinks before the crash and the decay time of n_e corresponds to τ_E (5-10ms).

The region of the appearance of the self-organized oscillation can be shown on the map of I_{FEI} and the value of $N_{//}$ of the additional LHW. The LHW with low $N_{//}$ has the preferable capability to the current drive and its current drive efficiency is better than that of the LHW with high $N_{//}$. The plasma with ITB can be achieved in the plasma with the additional LHW with $N_{//} < 2.4$. When the value of $N_{//}$ of the additional LHW is less than 2.4, it is difficult to make the plasma with ITB. When the value of influx of ferrite is larger than a certain value, it is difficult to maintain the plasma with ITB. However, SSSO can work on the assistance with the formation of ITB even in the high influx of ferrite as shown in Fig. 6. This indicates that SSSO plays an essential role in the exhaust of the metal impurities from the inside of ITB. This action of SSSO may work on the avoidance of the impurity accumulation and the dilution in steady state operation of fusion plasma with ITB.

5. Summary

ITB has been obtained in full LHCD plasmas on a superconducting tokamak, TRIMA-1M ($R=0.84m$, $a \times b=0.12m \times 0.18m$, $B_T < 8T$). The plasma with ITB can be maintained by the LH

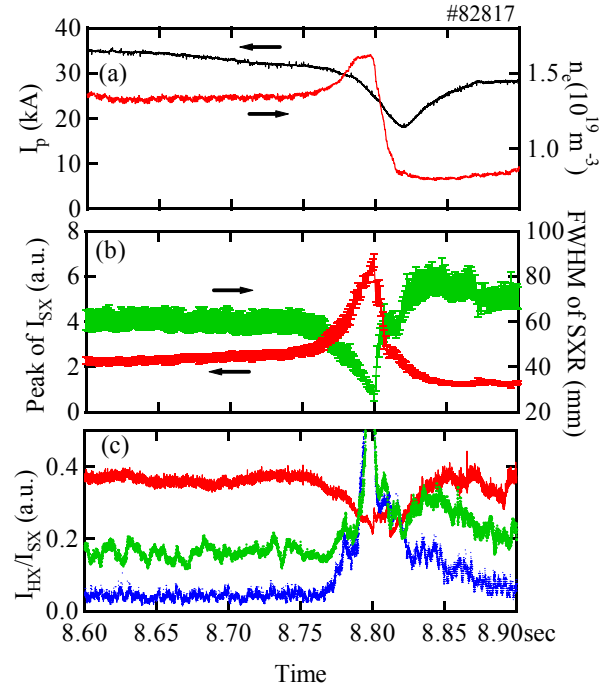


Fig. 5 Expanded figure around the crash of (a) I_p and n_e , (b) the peak value of I_{SX} profile and the full width of half maximum (FWHM) of I_{SX} profile, and (c) the ratio of I_{HX} to I_{SX} at $r=0cm$ (red line), 2.5cm (green line) and 5cm (blue line).

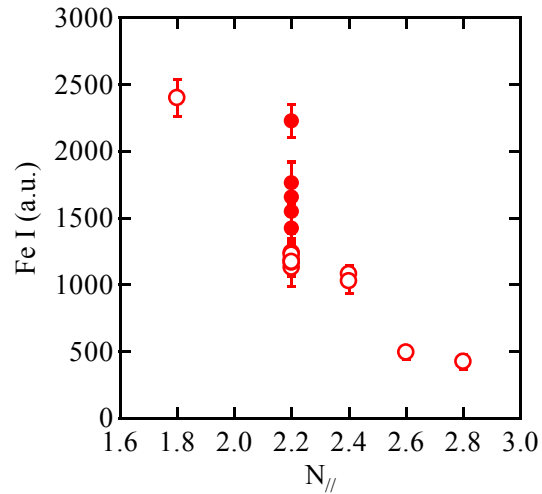


Fig. 6 The map on I_{FEI} and $N_{//}$ for the formation of ITB w/o SSSO (open circles) and with SSSO (closed circles).

power deposited around the foot point of ITB up to 25 sec, which corresponds to more than 100 times of current diffusion time, $\tau_{L/R}$. The metal impurity accumulation prevents us from maintaining the discharge with ITB for long time. The LH power deposited around ITB foot assists the formation of ITB and the LH power deposited at the center of the plasma obstacles it. This suggests that the hollow current profile is suitable to form ITB. Self-organized slow sawtooth oscillations (SSSO) of plasma current, density, temperature, and so on with the period comparable to the current diffusion time have been also observed in long duration full LHCD discharges. The oscillation appears only in the high performance plasma with ITB. The action of particle exhaust caused by SSSO is preferable to avoid the impurity accumulation. As the result the transition to the high performance plasma under the high influx of metal impurities can be obtained

6. Acknowledgement

This work has been partially performed under the framework of joint-use research in RIAM Kyushu University and the bi-directional collaboration organized by NIFS.

This work is partially supported by a Grant-in-Aid for Scientific Research from Ministry of Education, Science and Culture of Japan.

7. References

- [1] Wagner F, Fussmann G, Grave T, et al., PRL **53** (15) 1453-1456 (1984).
- [2] Koide Y, Kikuchi M, Mori M, et al., PRL **72** (23), 3662-3665 (1994)
- [3] Levinton FM, Zarnstorff MC, et al., PRL **75** (24), 4417-4420 (1995).
- [4] Strait EJ, Lao LL, Mauel ME, et al., PRL **75** (24): 4421-4424 (1995).
- [5] Turnbull AD, Taylor TS, Linliu YR, et al., PRL **74** (5), 718-721 (1995).
- [6] Gormezano C, Baranov YF, Challis CD, et al., PRL **80** (25): 5544-5547 (1998)
- [7] Fujita T, Ide S, Shirai H, et al., PRL **78** (12): 2377-2380 (1997).
- [8] G.T.Hoang et al, Nucl. Fusion **34**, 75 (1994).
- [9] Gruber O, Wolf RC, Dux R, et al., PRL **83**, 1787-1790 (1999).
- [10] Fujisawa A, Iguchi H, Minami T, et al., PRL **82** (13), 2669-2672 (1999).
- [11] Ohyabu N, Narihara K, Funaba H, et al., PRL **84** (1), 103-106 (2000).
- [12] Stroth U, Itoh K, Itoh SI, et al., PRL **86** (26), 5910-5913 (2001).
- [13] Ida K, Shimozuma T, Funaba H, et al., PRL **91** (8), 085003 (2003)
- [14] Naito O, Cui Z, Ide S, et al., PRL **89** (6), 065001 (2002).
- [15] Crisanti F, Litaudon X, Mailloux J, et al., PRL **88** (14), 145004 (2002).
- [16] Dux R, Giroud C, Zastrow KD, Nucl. Fusion **44** (2), 260-264 (2004)
- [17] Carraro L, Gabellieri L, Mattioli M, et al., Plasma Phys. Contrl. F. **46** (2), 389-407 (2004).
- [18] Giruzzi G, Imbeaux F, Segui JL, et al., PRL **91** (13), 135001 (2003)
- [19] S.Itoh, K.N.Sato, et al., Nucl. Fusion **39** (9Y) 1257-1270 (1999).
- [20] H.Zushi, et al., Nucl. Fusion Vol.41(10) (2001) 1483-1493.
- [21] K.Hanada, et al., Nucl. Fusion Vol.41(11) (2001) 1539-1542.
- [22] K.Hanada, et al., Journal of Plasma and Fusion Research Vol.77(3) (2001) 294-299